Engineering Geology 255 (2019) 59–68

Contents lists available at ScienceDirect

Engineering Geology

journal homepage: www.elsevier.com/locate/enggeo

Chemical and geotechnical properties of solidified/stabilized MSWI fly ash disposed at a landfill in China

Hui XU[a,b,*], Jiandong MIAO[a], Ping CHEN[a], Liangtong ZHAN[b], Yu-ze WANG[c]

[a] School of Civil Engineering and Architecture, Zhejiang Sci-Tech University, 2nd Street 928#, Hangzhou, China
[b] MOE Key Laboratory of Soft Soils and Geoenvironmental Engineering, Zhejiang University, Yuhangtang Road 866#, Hangzhou 310058, China
[c] Department of Engineering, University of Cambridge, Cambridge CB2 1PZ, UK

ARTICLE INFO

Keywords:
Solidified/stabilized MSWI fly ash
Geotechnical properties
Chemical properties
Aging effect
Landfill design and operation

ABSTRACT

The chemical and geotechnical properties of solidified/stabilized (s/s) municipal solid waste incineration (MSWI) fly ash are of prime importance for the design and operation of landfill sites. This study conducted field and laboratory tests to investigate aging effects on the chemical and geotechnical properties of s/s MSWI fly ash. Field investigations included borehole sampling and cone penetration tests (CPTs), and laboratory analyses included the measurement of the chemical, physical, hydrological, and mechanical properties of s/s fly ash with different fill ages. The results showed that: 1) Cl concentrations in landfill leachate were as high as 52,700 mg.L^{-1}, which may present a technical challenge for leachate treatment; 2) specific gravity decreased with fill age, which was attributed to the leaching of metal elements from the s/s fly ash; 3) mean particle size decreased with fill age, resulting in an increase in the gravimetric moisture retention capacity (MRC) and a decrease in the saturated hydraulic conductivity; 4) gravimetric MRC was much higher than the initial moisture content, suggesting water absorption by s/s fly ash after landfilling; and 5) shear strength decreased with fill age, which was consistent with the CPTs results. To improve the design and operation of s/s MSWI fly ash landfill sites, the following suggestions are made: 1) the use of concentrated MSW landfill leachate in the s/s fly ash process should be avoided to reduce the concentrations of subsequent landfill leachate; 2) leachate generation could be further reduced by improving landfill operation practices and by taking advantage of the absorption capacity of s/s fly ash; and 3) the specific geotechnical parameters of s/s fly ash should be obtained prior to the design of landfill sites, and their aging effects should also be taken into consideration.

1. Introduction

Incineration has been widely used due to its efficiency at reducing the volume of municipal solid waste (MSW) (Tang et al., 2016). However, incineration also has shortcomings, such as the production of MSWI fly ash, which is classified as a hazardous waste due to its high content of heavy metals including Cr, Cd, Pb, Hg, As, and Ni (Quina et al., 2008). It is estimated from data from the China Statistic Almanac that 1.5–3.7 million tons of MSWI fly ash was produced in China in 2016. China, along with other countries, requires that MSWI fly ash must be treated properly before its disposal in a sanitary landfill (Zhang et al., 2016). The harmless treatment methods of fly ash mainly include chemical stabilization, cement solidification, and thermal separation. Chemical stabilization and cement solidification have been widely adopted across the world due to their ease of application and high capabilities with respect to fixing heavy metals (Zacco et al., 2014).

The chemical and geotechnical properties of s/s MSWI fly ash are of prime importance for the design and operation of landfills. A full understanding of these properties is essential to address the geoenvironmental problems that can be associated with landfill sites, such as slope stability, landfill settlement, and leachate seepage and treatment. At present, many studies have been carried out to examine the leaching properties of s/s MSWI fly ash. Laboratory tests have demonstrated that the leachability of MSWI fly ash can be constrained within the standard limits when stabilized by chemical agents and/or solidified by cementitious materials (Jiang et al., 2004; Tang et al., 2016; Zhang et al., 2016). However, not much is known about the long-term chemical properties of s/s MSWI fly ash after it has been disposed at a landfill site. Besides, there is very limited literature on the geotechnical properties of s/s MSWI fly ash. Shimaoka and Hanashima (1996) conducted experiments using a large lysimeter filled with s/s fly ash together with MSW, finding that the mechanical strength of s/s fly ash left to stand

* Corresponding author at: School of Civil Engineering and Architecture, Zhejiang Sci-Tech University, 2nd Street 928#, Hangzhou, China
E-mail addresses: xuhui@zstu.edu.cn (H. XU), chenp@zstu.edu.cn (P. CHEN), zhanlt@zju.edu.cn (L. ZHAN), yw369@cam.ac.uk (Y.-z. WANG).

https://doi.org/10.1016/j.enggeo.2019.04.019
Received 10 October 2018; Received in revised form 26 April 2019; Accepted 29 April 2019
Available online 30 April 2019
0013-7952/

outdoors tended to reduce with time. Therefore, it is of great engineering significance to study the effects of aging on the chemical and geotechnical properties of s/s MSWI fly ash disposed at landfill sites.

This paper presents extensive field and laboratory investigations on the chemical and geotechnical properties of s/s MSWI fly ash obtained from a landfill in Nanjing, China. The fieldwork included borehole sampling, in situ leachate collection, and cone penetration tests (CPTs). The employed laboratory tests involved the measurement of the chemical properties of the landfill leachate, as well as the measurement of the chemical, physical, hydrological, and mechanical properties of s/s fly ash samples with different fill ages. The engineering implications of the results are also discussed with respect to the design and operation of s/s MSWI fly ash landfill sites.

2. Site description

The Jiangnan s/s MSWI fly ash landfill is located in Nanjing, China. Nanjing has high annual rainfall, approximating 1776 mm in 2016. The Jiangnan landfill was designed to operate in two phases: the first phase, put into operation in December 2015, has a storage capacity of 0.3 million m^3 with an operating period of 5 years; the second phase has a storage capacity of over 2.7 million m^3 with an operating period of > 25 years beginning in 2020. As shown in Fig. 1(a), the first phase was designed for construction in section I and II, and the second phase involves construction in section III as well as the vertical extension of section I and II.

The base structure of the first phase of the landfill site was designed to contain four zones according to the technical code for liner systems of municipal solid waste landfill sites (CJJ113-2007), as shown in Fig. 2. From top to bottom, the first zone was a leachate drainage and collection system (LDCS) composed of a layer of 200 g/m^2 geotextile, a 300 mm layer of gravel, and a double layer of 600 g/m^2 geotextile; the second zone was an impermeable system, which consisted of 2-mm thick high-density polyethylene (HDPE) geomembrane, a layer of geosynthetic clay liner (GCL), a 1.5-mm thick HDPE geomembrane, and a 500 mm layer of clay; the third zone was an underground water diversion system made up of a layer of 400 g/m^2 geotextile, a layer of 300 mm gravel and a layer of 200 g/m^2 geotextile; the fourth zone was the base layer for which the topsoil (silty clay) was 1.0–10.5 m with a

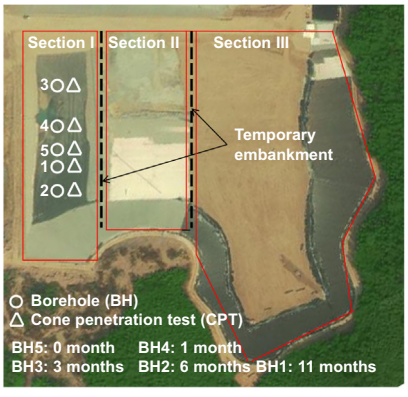

(a) Layout of boreholes and *in situ* CPTs

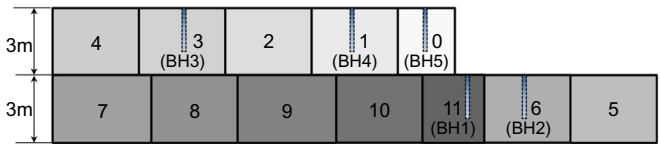

(b) Profile of section I

Fig. 1. Description of the investigated s/s MSWI landfill site.

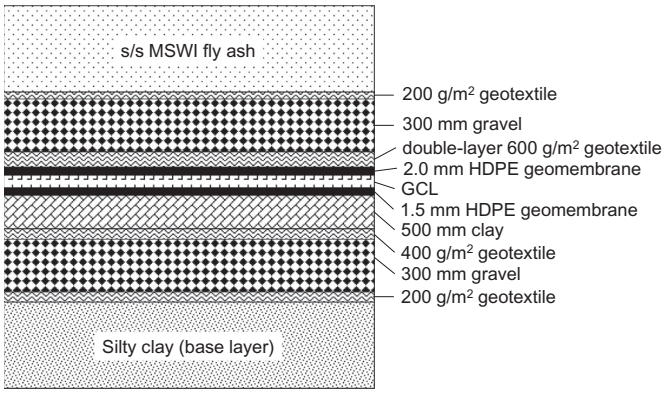

Fig. 2. Base structure profile of the investigated s/s MSWI landfill.

moisture content of 19.1–25.5% and a standard penetration test (SPT) blow count of 20–36. Up to November 2016, a total mass of 51,156 tons of s/s fly ash had been disposed of into the first phase of the landfill site at a rate of 100–200 t/d. Before being disposed of, the fly ash was stabilized/solidified using an organic chelator and lime, for which concentrated MSW leachate was used instead of water.

As requested by the landfill site operator, extensive field and laboratory investigations on the chemical and geotechnical properties of the s/s fly ash in the first phase of the site were carried out with the aim of providing further guidance for the design and operation of the second phase.

3. Materials and methods

3.1. Field investigation

The field study included borehole sampling, CPTs, and in situ leachate collection. Fig. 1 shows the layout of the boreholes and the CPT measurement locations and a cross-section view of the investigated landfill. The fill ages of the s/s MSWI fly ash from the boreholes (BH1 to BH5) were 11, 6, 3, 1, and 0 months, respectively. The drilling depth of the boreholes ranged from 0 to 2.0 m and the samples were taken using thin-walled samplers. Five CPTs (CPT1 to CPT5) were conducted to depths of 0 to 3.0 m in the vicinity of the five boreholes. The penetration rate of the cone was 1.2 m/min. Cone tip resistance and side friction were recorded at an interval of 0.1 m.

3.2. Chemical characterization of in situ landfill leachate and leaching solution of s/s fly ash

Two in situ landfill leachate samples were collected from the bottom drainage system of the Jiangnan landfill and four leaching solution samples were obtained from the s/s fly ash samples using the horizontal vibration method (HJ557-2010). Both sets of leaching solution samples had fill ages of 3 and 11 months. The chemical properties of both the leachate samples and the leaching solution samples were analyzed in certified laboratories. Seventeen indexes were analyzed in total for leachate samples, namely pH, chemical oxygen demand (COD), biological oxygen demand (BOD), ammonia nitrogen (NH_3-N), Cl, Ca, Mg, K, Cu, Zn, Pb, Cd, Ba, Hg, Ni, As, and Cr. The leaching solution samples were analyzed for Ca, Cu, Zn, Pb, and Cd. The analyses were conducted using standardized determination methods—generally the standards from the China Ministry of Environmental Protection (China MEP) and the United States Environmental Protection Agency (US EPA), as shown in Table 1.

Table 1
Indexes, determination methods, and units of the chemical characterization tests.

Indexes	Determination method	Unit
pH	GB 6920	–
COD	GB/T 11914	mg L^{-1}
BOD	HJ 505	mg L^{-1}
NH_3-N	HJ 535	mg L^{-1}
Cl	HJ/T 84	mg L^{-1}
Ca	USEPA 200.7	mg L^{-1}
Mg	USEPA 200.7	mg L^{-1}
K	USEPA 200.7	mg L^{-1}
Cu	USEPA 200.8	mg L^{-1}
Zn	USEPA 200.8	mg L^{-1}
Pb	USEPA 200.8	mg L^{-1}
Cd	USEPA 200.8	mg L^{-1}
Ba	USEPA 200.8	mg L^{-1}
Hg	HJ 597	mg L^{-1}
Ni	USEPA 200.8	mg L^{-1}
As	USEPA 200.8	mg L^{-1}
Cr	USEPA 200.8	mg L^{-1}

3.3. Mechanical characterization of s/s fly ash

3.3.1. Measurement of physical properties

The particle size distribution of dry s/s fly ash samples was determined by sieving. The water content—defined as the mass ratio of water to dry sample—was determined using oven drying. Specific gravity was measured by the combination of a density-pyknometer (for particle sizes < 5 mm) and the suspension method (for particle sizes > 5 mm). In specific gravity tests, kerosene was used instead of water as s/s fly ash contains a large amount of dissolved minerals. All the above tests were carried out according to the Chinese specification for soil testing (SL237–1999). The physical properties of raw fly ash sampled from the local MSWI plant were also measured according to the described methods.

3.3.2. Measurements of hydrological and compression properties

Compression, moisture retention capacity (MRC), and hydraulic conductivity tests were carried out in a self-designed compression cell, as shown in Fig. 3. The cylinder was made from polymethyl methacrylate, having a height of 20 cm and an inside diameter of 10 cm. A hydraulic system was designed to drain liquid via the water inlet/outlet at the bottom of the cell and to saturate the specimen from the bottom to the top. Vertical stresses were applied to the specimens via an air loading system. The tests were carried out in the following steps. First, the dry sample was filled into the cylinder and then compacted manually to reach a certain thickness. Next, initial vertical stress was applied to the sample and maintained for 24 h for the compression test. During this period, settlement was measured using a dial indicator. Subsequently, the load plate was removed, the sample was saturated, and a constant hydraulic head (hydraulic gradient of approximately 2.0) was applied by using a Markov bottle for the hydraulic conductivity test. When a steady state of flow had been established, the liquid flow was recorded. After the completion of the hydraulic conductivity test, the bottom pipe was shifted to connect to a measuring cup using a three-way valve, and the water that flowed out from the saturated sample under gravity was collected. When the collected outflow liquid per day was < 0.1% of the sample mass, the sample was considered to have reached its MRC. At that time, the first round of tests was completed and the second round of tests was conducted by repeating the above steps, starting with the application of the second vertical stress. The vertical stress increments applied in this study were 0, 50, 100, 200, and 400 kPa.

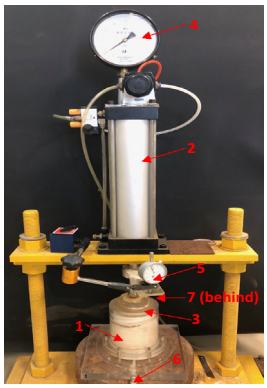

1 = test cylinder, 2 = air-loading system, 3 = load plate, 4 = pressure gauge, 5 = dial indicator, 6 = water inlet/outlet, 7 = water outlet

Fig. 3. Compression cell.

3.3.3. Triaxial compression test

The consolidated drained triaxial compression test was performed by using a strain control triaxial compression apparatus (STSZ-2, Jianke Instrument Co., LTD, China). The molded samples were 61.8 mm in diameter and 125 mm in height, prepared with the following in situ unit weight of s/s fly ash: 11.1, 12.3, 11.2, 11.0, and 11.8 kN/m^3 for BH5, BH4, BH3, BH2, and BH1, respectively. Initial saturation was achieved by percolating degassed water through each sample. Further saturation was accomplished through the application of confining pressure and backpressure, specifically 100, 200, 300, and 400 kPa. The strain rate for the drained shearing tests was 0.1 mm/min. The peak deviatoric stress was determined as the shear strength at a given confining pressure, and cohesion and friction angle were determined using the Mohr-Coulomb failure criterion.

4. Results and analysis

4.1. Description of the borehole samples

During the drilling process, the samples taken at a depth of 0–0.5 m were found to be darker in color than those taken from a depth of 1.5–2.0 m (Fig. 4). This suggests that rainfall has infiltrated into the shallow layer. In addition, some large size particles were found in the borehole samples (circled in red line in Fig. 4), which may result from the cementing effect of the lime that was added in the s/s fly ash process. However, some of the large size particles were broken into small particles after drying, but some were not, which may be related to the different degrees of cementation. In the following sections, the geotechnical test results mainly focus on the samples taken at a depth of 0–0.5 m for following two reasons: 1) not all the geotechnical tests could be conducted on the deeper samples due to a limited number of samples; and 2) the properties of s/s fly ash at shallower depths tend to be significantly influenced by the landfill environment (Shimaoka and Hanashima, 1996) and, therefore, have more academic value and should have more attention paid to them.

4.2. Leaching characteristics

The chemical properties of the leachate samples and leaching solution of s/s fly ash samples with fill ages of 3 and 11 months are summarized in Table 2. The pH of the leachate was 9.25 and the NH_3-N concentration was 87.9 mg L^{-1}. The high alkalinity of the leachate was mainly due to the ammonium hydroxide spray applied for denitration in the flue-gas-disposing system and the addition of lime to the fly ash during the s/s process. The COD and BOD of the leachate were approximately 1155.1 mg L^{-1} and 446.5 mg L^{-1}, respectively. The concentration of Cl in the leachate was as high as 52,700 mg L^{-1}, which was mainly associated with a high content of food waste and plastic

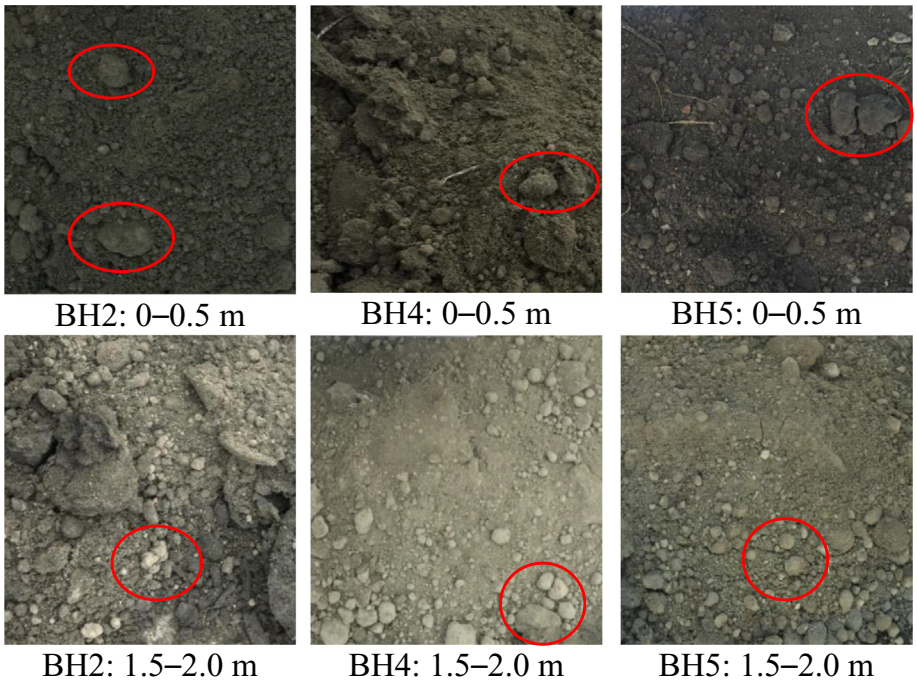

Fig. 4. Photographs of samples obtained from BH2, BH4 and BH5.

materials in the MSW. However, effective wastewater treatment to reduce high Cl concentrations can be challenging (Spence and Shi, 2005; Colangelo et al., 2012). The concentration of Ca in the leachate was 6585 mg L^{-1}, which is much higher than in MSW landfill leachate (Fan et al., 2006). The high concentration of Ca may induce the precipitation of a large amount of calcium carbonate, which can consequently result in serious clogging of the LDCS. Hard $CaCO_3$ that causes clogging should, if possible, be avoided by keeping organic content low in the leachate. The concentrations of the heavy metals Hg, Cu, Zn, Pb, Cd, Ba, Ni, As, and Cr, were all below the Chinese Standard for Pollution Control on the Landfill Site of Municipal Solid Waste (GB 16889–2008).

With the exception of Ca, the concentrations of the heavy metals in the leaching solution of s/s fly ash samples were much higher than in the landfill leachate. It should be noted that the replacement of water with concentrated MSW landfill leachate in the s/s fly ash process may have contributed to these high concentrations. In addition, it was found that the leaching concentrations of heavy metals from 11-month s/s fly ash samples were lower than those of 3-month samples. This was probably due to the dissolution and removal of heavy metals via rainfall infiltration and percolation through the landfill materials, meaning that the extent of heavy metal leaching increased—and the amount retained in the s/s fly ash decreased—with fill age.

4.3. Physical properties

4.3.1. Particle size distribution

The particle size distribution curves of the s/s fly ash together with the raw fly ash are shown in Fig. 5. For the s/s fly ash, the fraction of fine particles (< 0.075 mm) was almost 0% and the > 4.75 mm size class accounted for 14–30% of the samples. Values obtained for the non-uniform coefficient C_u and the curvature coefficient C_c were in the range of 4.56–10.33 and 0.32–0.43, respectively. According to the

Table 2
Chemical properties of landfill leachate and s/s fly ash leaching liquid.

Indexes	Landfill leachate	s/s fly ash leaching liquid		Limits[a]
		3 months	11 months	
pH	9.25 ± 0.11	–	–	–
COD (mg L^{-1})	1155.1 ± 115	–	–	–
BOD (mg L^{-1})	446.5 ± 35.5	–	–	–
NH_3-N (mg L^{-1})	87.9 ± 0.5	–	–	–
Cl (mg L^{-1})	52,700 ± 2500	–	–	–
Ca (mg L^{-1})	6585 ± 845	474 ± 87	145.8 ± 34	–
Mg (mg L^{-1})	10.1 ± 0.5	–	–	–
K (mg L^{-1})	12,550 ± 1450	–	–	–
Cu (mg L^{-1})	0.004 ± 0.002	0.056 ± 0.011	0.027 ± 0.007	40
Zn (mg L^{-1})	0.009 ± 0.002	4.61 ± 0.58	3.49 ± 0.52	100
Pb (mg L^{-1})	0.003 ± 0.001	0.168 ± 0.043	0.028 ± 0.006	0.25
Cd (mg L^{-1})	< 0.0001	0.00085 ± 0.00016	0.00015 ± 0.00005	0.15
Ba (mg L^{-1})	2.3 ± 0.37	–	–	25
Hg (mg L^{-1})	< 0.0001	–	–	0.05
Ni (mg L^{-1})	0.002 ± 0.0003	–	–	0.5
As (mg L^{-1})	< 0.005	–	–	0.3
Cr (mg L^{-1})	0.002 ± 0.001	–	–	4.5

[a] limit values from Chinese standard for pollution control on the landfill site of municipal solid waste (GB16889-2008).

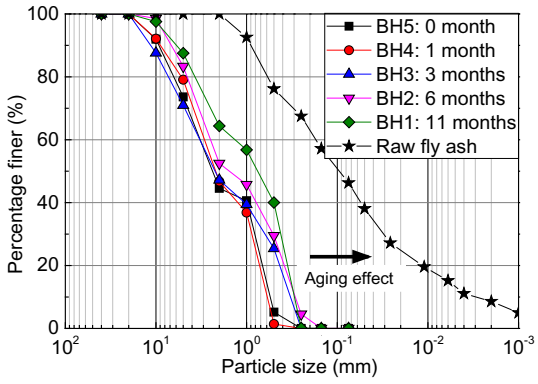

Fig. 5. Particle size distribution of s/s fly ash (0–0.5 m).

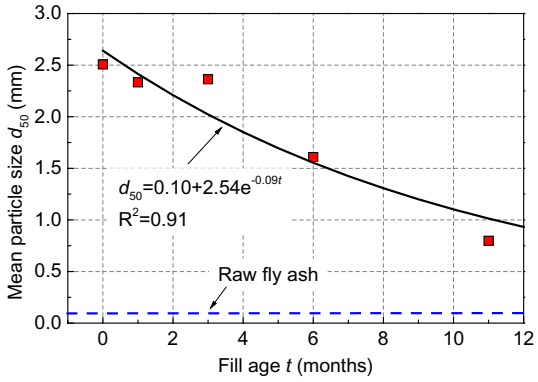

Fig. 6. Variation in mean particle size with fill age for s/s fly ash (0–0.5 m).

Unified Soil Classification System (USCS, ASTM D2487-11), the s/s fly ash was classified as poorly graded sand. The particle size of the s/s fly ash also tended to decrease with age, progressing towards a similar particle size distribution as the raw fly ash. The mean particle size d_{50} of s/s fly ash was in the range of 0.8–2.5 mm, which clearly decreased with fill age (Fig. 6). A regression analysis between the d_{50} and fill age (t) obtained the model: $d_{50} = 0.10 + 2.54\exp(-0.09\,t)$, where $R^2 = 0.91$. The aging effect on particle size may be caused by the cementitious deterioration of s/s fly ash under seasonal wetting and drying and changes in temperature (Shimaoka and Hanashima, 1996). With respect to the particle sizes of MSW materials, decreases have also been observed with fill age, although this is thought to be related to the biodegradation of organic matter (Hossain et al., 2009).

4.3.2. Specific gravity

The specific gravity of s/s fly ash decreased from 2.56 to 1.68 in the 0-month and 11-month samples, respectively (Fig. 7). The relationship between specific gravity (G_s) and fill age (t) was described as: $G_s = 1.51 + 1.06\exp(-0.15\,t)$, where $R^2 = 0.95$. The specific gravity of fresh s/s fly ash (0 months) was close to that of raw fly ash (2.46–2.58). Hence, the decrease of s/s fly ash specific gravity with age is possibly related to the leaching of metal elements as described in Section 4.2. With the increase of fill age, more metal elements are leached out and, therefore, the specific gravity of s/s fly ash is decreased. A similar phenomenon has been observed in cementitious materials due to the dissolution of Ca (Chiu, 2009).

Typical values of specific gravity for most soils range from 2.60 to 2.80 (Holtz et al., 2011; Federico et al., 2018; Feng et al., 2017a; Zhai et al., 2018), which is slightly higher than that observed for s/s fly ash. This is mainly attributed to the presence of hollow particles in the fly ash (Reddy et al., 2018). The average specific gravity reported for fresh uncompacted and compacted MSW is 1.072 and 1.258, respectively, and 2.201 for old MSW (Yesiller et al., 2014). Thus, the specific gravity

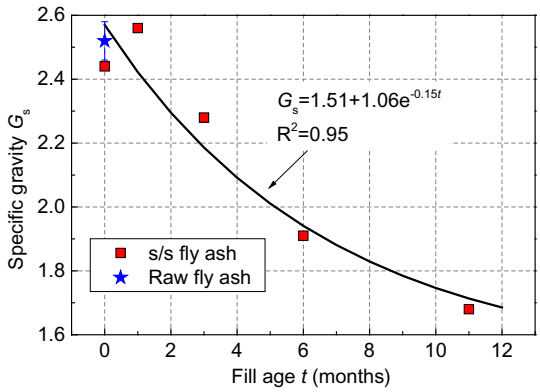

Fig. 7. Variation in specific gravity with fill age for s/s fly ash (0–0.5 m).

of MSW is increased in the landfill environment over time—showing the opposite trend to s/s fly ash.

4.3.3. Moisture content

The moisture content of the s/s fly ash samples obtained from BH5, BH4, BH3, BH2, and BH1 was 47.3%, 46.5%, 48.9%, 61.6%, and 86.4% for, respectively. It should be noted that the initial moisture content of the s/s fly ash before landfilling was much lower, in the range of 17.6–19.9%. This increase in moisture content is mainly attributed to rainfall infiltration post-landfill.

The initial moisture content of MSW from the cities of Hangzhou, Shanghai, and Suzhou has been reported to be approximately 144%, 132%, and 156%, respectively (Lan et al., 2012), which is significantly higher than for s/s fly ash. This is mainly attributed to Chinese MSW having a high food waste content containing a large amount of intra-particle water (Zhan et al., 2017). After landfilling, most of the intra-particle water in MSW is released within a few months due to the rapid hydrolysis of food waste, and also via compression under upper waste layers (Zhan et al., 2017; Xu et al., 2016). As a result, the moisture content of aged MSW from Hangzhou, Shanghai, and Suzhou decreased to 40 ± 20%, 48.5 ± 15.5%, and 85 ± 55%, respectively, following its disposal to landfill (Zhu et al., 2004; Zhan et al., 2008; Feng et al., 2017b). The moisture content of aged MSW is, therefore, typically lower than it is initially—which is the opposite trend to s/s fly ash.

4.4. Hydrological properties

4.4.1. Moisture retention capacity (MRC)

A significant variation in gravimetric MRC values was observed in the s/s fly ash samples with different fill ages, ranging from 17.7% to 110.1% (Fig. 8). The highest MRC values belonged to the sample with

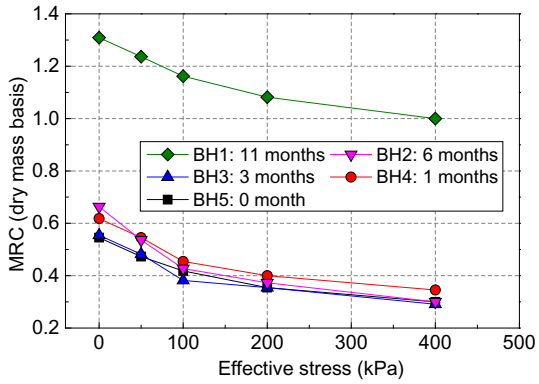

Fig. 8. Variation in gravimetric MRC with effective stress for s/s fly ash (0–0.5 m).

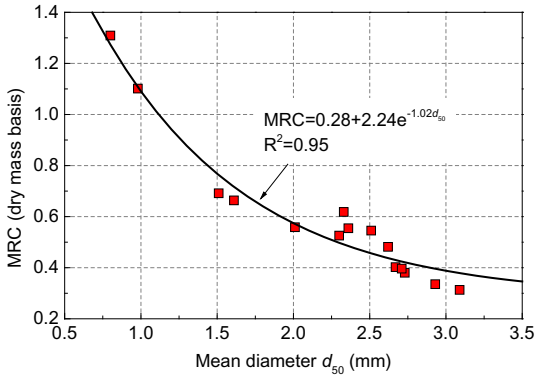

Fig. 9. Variation in gravimetric MRC with mean particle size for s/s fly ash (0–0.5 m, 0.5–1.0 m, and 1.5–2.0 m). All data were determined at a stress level of 0 kPa.

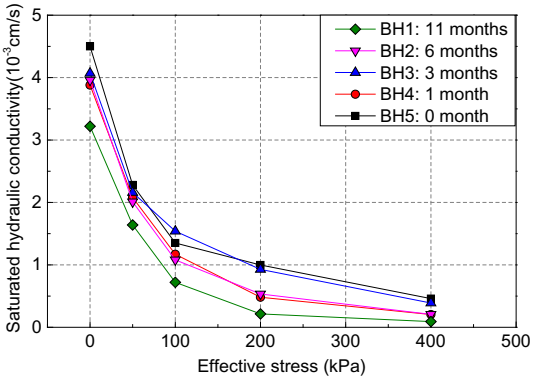

Fig. 11. Variation in saturated hydraulic conductivity with effective stress for s/s fly ash (0–0.5 m).

fill age of 11 months, which was associated with its small particle size. As shown in Fig. 9, MRC values decreased significantly with mean particle size (d_{50}), giving the regression model: MRC = 0.28 + 2.24exp ($-1.02d_{50}$), where $R^2 = 0.95$. That is, samples with a smaller mean particle size have a larger specific surface area and, as a result, have a higher MRC. It was also observed that the initial moisture content of s/s fly ash (17.6–19.9%) was much lower than the MRC values. Therefore, s/s fly ash has the capacity to absorb water after being placed in a landfill site. In contrast, MSW in China has a much higher initial moisture than MRC (Xu et al., 2016). Therefore, MSW produces a significant amount of self-released leachate after landfilling (Zhan et al., 2017).

The variations in volumetric MRC with porosity for typical soils and s/s fly ash are summarized in Fig. 10. Overall, the volumetric MRC of typical soils tends to increase with increasing porosity. The volumetric MRC of typical soils can be classified into three ranges, specifically 6–23% (sand), 23–38% (silt), and 38–58% (clay). This can also be explained by the particle size effects outlined above. The volumetric MRC values obtained in this study for s/s fly ash were within the ranges for silt and clay, and exhibited a clear increasing trend with porosity.

4.4.2. Saturated hydraulic conductivity

The saturated hydraulic conductivity of the s/s fly ash decreased significantly with increasing effective stress (Fig. 11). For example, the saturated hydraulic conductivity of the BH1 sample decreased from 3.2×10^{-3} cm/s to 9.1×10^{-5} cm/s when effective stress was increased from 0 kPa to 400 kPa. This was mainly due to a reduction in inter-particle voids under the increasing effective stress. In addition, the saturated hydraulic conductivity decreased with fill age at a given effective stress. For example, at an effective stress of 0 kPa, the saturated hydraulic conductivity of the 0-month to 11-month samples decreased from 4.5×10^{-3} cm/s to 3.2×10^{-3} cm/s, respectively. This was mainly attributed to the decrease in particle size with aging.

The Kozeny-Carman model (Taylor, 1948) and the logarithmic model (Mesri and Olson, 1971) are two commonly applied methods of predicting the saturated hydraulic conductivity of porous media when considering the effects of porosity. Based on the test results, the relationship between the saturated hydraulic conductivity (k_s) and the void ratio (e) for s/s fly ash was characterized by the following two models (Fig. 12): $k_s = 0.001e^3 / (1 + e)$, where $R^2 = 0.698$ (Kozeny-Carman model); and $\lg(k_s) = 4.4325 \lg(e) - 3.9115$, where $R^2 = 0.753$ (logarithmic model). Both of these models captured the variation in k_s with respect to e for the s/s fly ash samples fairly well, with the logarithmic model performing slightly better.

Typical relationships between k_s and e for sand ($d_{10} = 0.1$ mm, Chapuis, 2004), silty sand ($d_{10} = 0.01$ mm, Chapuis, 2004), clay (specific gravity $G_s = 2.75$ and specific surface area $S_S = 60\ m^2/g$, Chapuis and Aubertin, 2003), and MSW (Xu et al., 2014) are also presented in Fig. 12. It can be observed that the results obtained for s/s fly ash fall between the curves for silty sand and clay, which is similar to the volumetric MRC data. In addition, the s/s fly ash data were all below the curve for MSW, suggesting a relatively lower hydraulic conductivity at a given porosity. In addition, the reduction rate of k_s with decreasing e was much smaller for s/s fly ash than for MSW. This might be associated with the void blocking effect caused by flexible materials (i.e., plastic bags) contained within MSW.

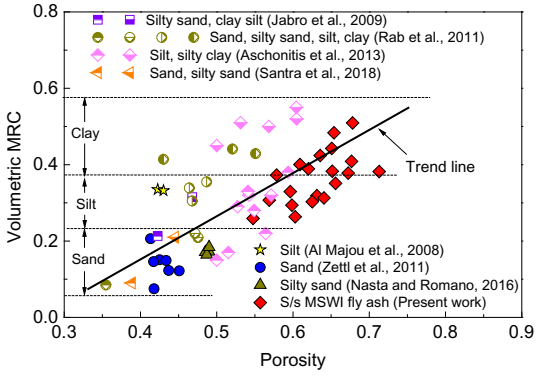

Fig. 10. Variation in volumetric MRC with porosity for different materials (Al Majou et al., 2008; Aschonitis et al., 2013; Jabro et al., 2009; Rab et al., 2011; Nasta and Romano, 2016; Santra et al., 2018; Zettl et al., 2011).

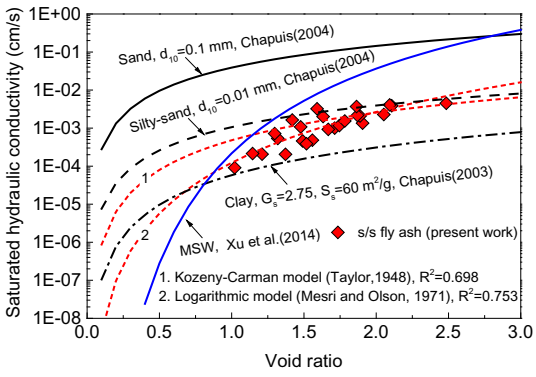

Fig. 12. Variation in saturated hydraulic conductivity with void ratio for different materials.

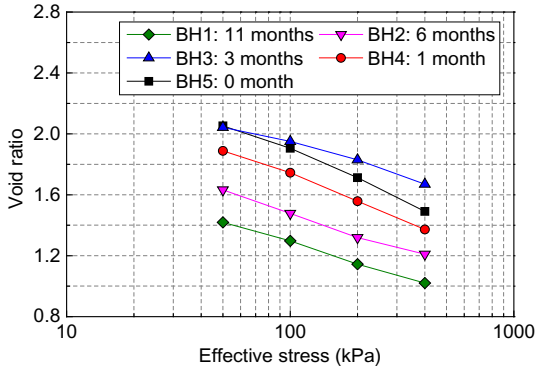

Fig. 13. Variation in void ratio with effective stress for s/s fly ash (0–0.5 m).

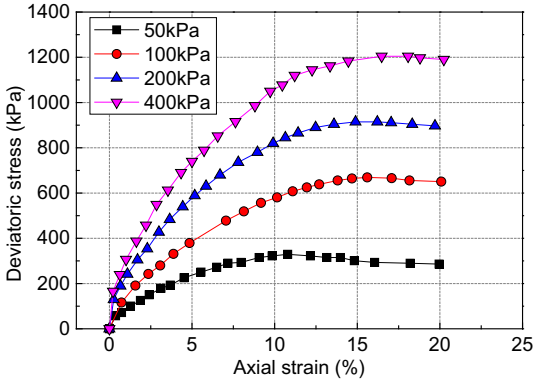

Fig. 15. Stress-strain curves of s/s fly ash (BH3, 0–0.5 m).

4.5. Mechanical properties

4.5.1. Compressibility

The void ratio of s/s fly ash decreased linearly with the logarithm of effective stress (Fig. 13). The compressibility of the samples was quantified in terms of the modified compression index C_c', which is defined as $C_c' = C_c / (1 + e_0)$, where C_c is the gradient of the e-log (σ'_v) curve and e_0 is the initial void ratio of the samples. The calculated values of C_c' for s/s fly ash were in the range of 0.13–0.18, with an average value of 0.16. These values are comparable to those of the low-plasticity clayey soils (Yu et al., 2007; Chai and Carter, 2011; Georgiannou et al., 2018) and aged MSWs (Machado et al., 2002; Bareither et al., 2012); are lower than high-plasticity clayey soils (Almeida et al., 2000; Huang et al., 2006; Zeng et al., 2017) and fresh MSWs (Stoltz et al., 2010; Zhan et al., 2017); and are slightly higher than non-crushable sands (Sanzeni et al., 2012; Wils et al., 2015).

The rate of primary consolidation, quantified in terms of the coefficient of consolidation (c_v), was determined by the square-root of time fitting method. The variation of the consolidation coefficient with effective stress for s/s fly ash is shown in Fig. 14. The values of c_v ranged from 0.77 cm^2/s to 0.95 cm^2/s under the effective stress of 50 kPa, and decreased significantly to 0.11–0.25 cm^2/s at 400 kPa. These c_v values for s/s fly ash are much higher than for clays (Vinod and Sridharan, 2015; Yu et al., 2016) and MSWs (Siddiqui et al., 2013; Babu and Lakshmikanthan, 2015), and are lower than for sands (Brennan and Madabhushi, 2010; Ecemis et al., 2015).

4.5.2. Shear strength

The typical stress-strain curves for the sample obtained from BH3 are shown in Fig. 15. The four curves—which correspond to the confining pressures of 50, 100, 200 and 400 kPa—exhibited a similar trend. In each case, the deviatoric stress increased rapidly to its peak value and then tended to decrease as the axial strain increased, indicating a strain-softening behavior. The peak values obtained were 329, 669, 915, and 1204 kPa at confining pressures of 50, 100, 200, and 400 kPa, respectively. The corresponding axial strains were 10.8%, 15.6%, 14.9%, and 16.5%, respectively. These data indicated that the axial strain at the peak deviatoric stress increased with confining pressure.

The correlations between shear strength parameters (i.e., cohesion (c) and friction angle (ϕ)) and the fill age of s/s fly ash are shown in Fig. 16. The values of cohesion and friction angle decreased from 34.1° and 19.5 kPa to 32.9° and 14.0 kPa, respectively, with increasing of fill age (from 0 to 11 months). The regression models obtained were: $c = 13.8 + 5.7\exp(-0.18\,t)$, where $R^2 = 0.95$; and $\phi = 32.4 + 1.7\exp(-0.10\,t)$, where $R^2 = 0.73$. As stated in Section 4.3.1, the particle size of the s/s fly ash was similar to poorly graded sand. With respect to particle size distribution, the s/s fly ash should have a cohesion value close to zero, as is the case for sand. However, the measured values of cohesion of the s/s fly ash were much higher than zero. This might be associated with the cementing effect from both the raw fly ash and the lime added in the s/s process. The reduction of cohesion with fill age might be associated with the cementitious deterioration of the s/s fly ash due to seasonal wetting and drying and changes in temperature (Shimaoka and Hanashima, 1996). In addition, the reduction in the friction angle with increasing fill age can be explained by considering particle size. As shown in Fig. 17, the friction angle of s/s fly ash decreased linearly with the decreasing logarithmic mean of particle size. This trend has also been observed in typical soils, as shown in Fig. 17. The friction angle of s/s fly ash fell in between unweathered and weathered soils at a given d_{50}. This may be associated with the strength of s/s fly ash particles being lower than the unweathered soil particles and higher than the weathered soil particles. In addition, and contrary to the s/s fly ash, the friction angle of MSW was found to decrease with increasing mean particle size. As for MSWs, large-size fibrous materials

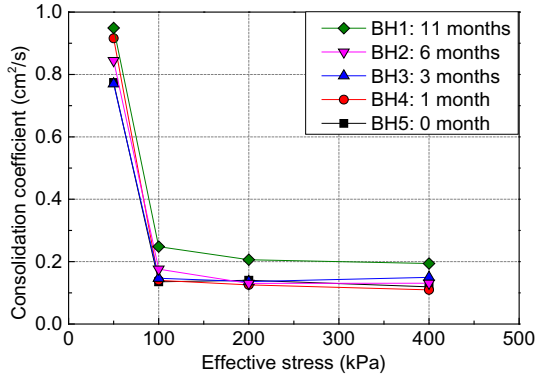

Fig. 14. Variation in consolidation coefficient with effective stress for s/s fly ash (0–0.5 m).

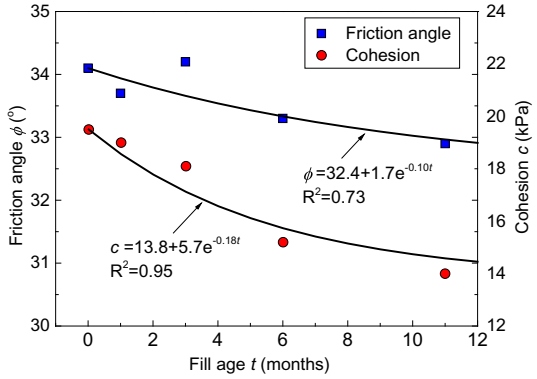

Fig. 16. Variation in cohesion and friction angle with fill age for s/s fly ash (0–0.5 m).

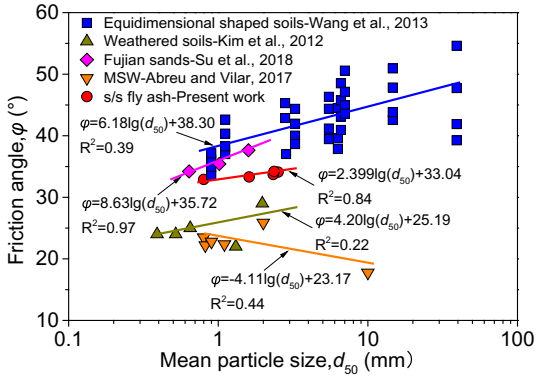

Fig. 17. Variation in friction angle with mean particle size for different materials (Abreu and Vilar, 2017; Kim and Lim, 2012; Su et al., 2018; Wang et al., 2013).

(e.g., food and garden wastes) can be decomposed into small-sized soil-like materials, which possess higher frictional resistance than fibrous materials (Zhan et al., 2008).

4.5.3. Penetration resistance

Tip resistance (q_c), side friction (f_s), and friction ratio (f_s/q_c) values obtained from the CPTs are plotted against penetration depth (0–3.0 m) in Fig. 18. The values of q_c ranged from 1 to 7 MPa, with the majority falling between 1 and 4 MPa. The average tip resistance for CPT5, CPT4, CPT3, CPT2, and CPT1, which was calculated from the arithmetic averages of q_c within the depth range of 0 to 3.0 m, was 3.2, 2.7, 3.9, 2.1, and 1.4 MPa respectively. The average tip resistance values tended to decrease with fill age, which tallies with the shear strength measurements obtained from the laboratory triaxial compression tests. However, the opposite trend has been observed at MSW landfill sites (Zhan et al., 2008; Machado et al., 2010). This difference is explained by the fact fibrous materials are decomposed into soil-like materials during the degradation of MSWs, which possess higher frictional resistance. The values of f_s ranged from 10 to 120 kPa, with the majority falling between 10 and 80 kPa. It should be noted that q_c and f_s values for CPT3 were relatively high among the five cores, probably as a result of a larger friction angle and larger particle sizes. The variation in f_s/q_c between the five cores ranged from 1% to 4%, which is comparable to the data from MSW landfill sites (Zhan et al., 2008; Machado et al., 2010). According to soil classification charts presented in Eslami and Fellenius (2004), the penetration resistance behavior of s/s fly ash is similar to the soil types from silty clay to silty sand.

5. Engineering implications for s/s MSWI fly ash landfills

In China, the construction of landfills specifically for s/s MSWI fly ash began several years ago; however, due to a lack of operational experience and technical standards, the designs for s/s MSWI fly ash landfill sites commonly follow the same specifications as MSW landfill sites. The chemical and geotechnical properties of s/s MSWI fly ash are, however, notably different from MSW. Appropriate guidelines for the design and operation of s/s MSWI fly ash landfills are, therefore, sorely need.

The concentrations of Ca, Cl, and heavy metals in the leachate of s/s fly ash landfills are much higher than in the leachate of MSW landfills (Fan et al., 2006; Long et al., 2018). Treatment technologies for dealing with leachate from the s/s fly ash landfills would, therefore, be challenging and expensive, and the high concentration of Ca also tends to induce serious clogging of LDCSs. These issues can be addressed in the following ways. Firstly, the use of concentrated MSW landfill leachate instead of water in the s/s fly ash process contributes to higher concentrations of Cl, COD and heavy metals, in the leachate produced from s/s fly ash landfill sites. Therefore, this approach should be avoided and this recommendation should be appended in the Chinese technical standard for s/s treatment of fly ash. Secondly, s/s fly ash has the capacity to absorb water after being disposed of at landfill sites, which is in contrast to typical Chinese MSWs. Hence, leachate is seldom produced from s/s fly ash itself but is instead mainly derived from rainfall infiltration. One approach to reducing the generation of leachate would, therefore, be to increase the level of cover over landfill sites and to avoid disposing of s/s fly ash on rainy days. By doing so, the capacity and costs of leachate disposal plants would be significantly reduced. In addition, the adverse effects of the cementitious deterioration of s/s fly ash would be mitigated due to a reduction in rainfall infiltration.

The geotechnical properties of s/s fly ash were found to be quite different from MSW materials and one specific type of typical soil. According to its particle size distribution, the studied s/s fly ash was classified as poorly graded sand, yet its cohesion was much higher than zero. The saturated hydraulic conductivity was found to fall between silty sand and clay at any given porosity, and the consolidation

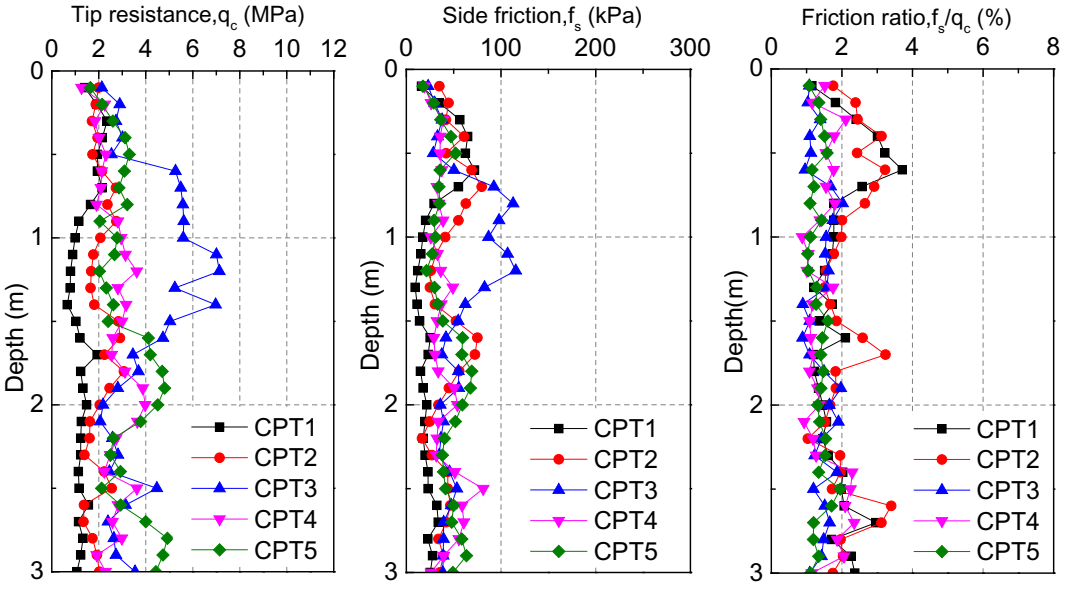

Fig. 18. Results of CPTs (CPT1 = 11 months; CPT2 = 6 months; CPT3 = 3 months; CPT4 = 1 month; CPT5 = 0 month).

coefficient was greater than clay and lower than sand. The MRC value was within the ranges of silt and clay, and the penetration resistance behavior was similar to silty clay to silty sand soils. The most important observed difference was that the geotechnical properties of s/s fly ash substantially changed with fill age, whereas aging effects are insignificant for typical soils. As a degradable material, the effects of aging on the geotechnical properties of MSWs are also considerable. The specific gravity, friction angle, and penetration resistance of MSWs increased over time, but these trends were opposite for s/s fly ash. Therefore, the geotechnical parameters for s/s fly ash should be obtained prior to the design of a s/s fly ash landfill site, while the application of parameters for MSW materials or typical soils would probably result in significant deviations in the design. In addition, in the assessment of geoenvironmental issues, such as slope stability, landfill settlement, leachate generation, and seepage, the effects of aging on the physical, hydrological, and mechanical properties of s/s fly ash should be taken into consideration. It is important and urgent to develop a technical standard specifically for s/s MSWI fly ash landfill sites in many countries, including China, that covers structural design, engineering construction, pollution control, operation, and maintenance.

6. Summary and conclusion

Understanding of the chemical and geotechnical properties of s/s MSWI fly ash is essential for the design and operation of landfill sites. However, not much is known about the long-term chemical and geotechnical behaviors of s/s MSWI fly ash disposed at landfill sites. Thus, this study carried out field and laboratory investigations to characterize the effects of aging on the chemical and geotechnical properties of s/s MSWI fly ash. The findings are summarized as follows:

(1) Chemical properties: The concentrations of Cl in landfill leachate were as high as 52,700 mg L^{-1}, which presents a technical challenge for leachate treatment. The concentration of Ca in leachate reached 6585 mg L^{-1}, which tends to induce serious clogging of LDCSs. The leaching concentrations of heavy metals from s/s fly ash tended to decrease with fill age and, with the exception of Ca, were much higher than in landfill leachate.
(2) Physical properties: The particle size distribution was similar to the poorly graded sand according to the USCS. Mean particle size and specific gravity were in the ranges of 0.8–2.5 mm and 1.68–2.56, respectively, and both tended to decrease with fill age. The initial moisture content was 17.6–19.9%, which is much lower than that after landfilling (46.5–86.4%).
(3) Hydrological properties: Gravimetric MRC was higher than the initial moisture content, suggesting a propensity to absorb water. Saturated hydraulic conductivity decreased from 10^{-3} cm/s to 10^{-4} cm/s with an increase in effective stress from 0 kPa to 400 kPa. Gravimetric MRC increased and saturated hydraulic conductivity decreased with a decrease in mean particle size, i.e., with increasing fill age.
(4) Mechanical properties: The modified compression index ranged from 0.13 to 0.18 and the consolidation coefficient was in the order of 10^{-1} cm^2/s. The stress-strain curves showed a strain-softening behavior. The cohesion and friction angle were in the ranges of 14.0–19.5 kPa and 32.9–34.1° respectively, and both tended to decrease with fill age. The effect of aging on shear strength was consistent with the field CPTs results. The CPTs yielded in a friction ratio in the range of 1% to 4%.

Based on these findings, the following suggestions are made to inform the design, operation, cost-effectiveness, and environment friendliness s/s MSWI fly ash landfill sites: (1) the replacement of water with concentrated MSW landfill leachate should be avoided in the s/s fly ash process to reduce resulting leachate concentrations; (2) leachate generation could be reduced by taking advantage of the water absorption capacity of s/s fly ash and by improving landfill operation practices, such as enhancing cover systems and avoiding landfill activities on rainy days; and (3) geotechnical parameters for s/s fly ash should be obtained prior to the design of landfill sites and the effects of aging should also be taken into consideration.

Acknowledgments

The authors are very grateful for the financial support of the National Natural Science Foundation of China (Grant Nos. 51578508 and No. 51708508), the Ministry of Housing and Urban-Rural Development of China (Grant No. 2015R3002) and the Science Technology Department of Zhejiang Province (Grant No. 2019C03107). The authors would also like to express their deep thanks to the reviewers for their constructive comments.

References

Abreu, A.E.S., Vilar, O.M., 2017. Influence of composition and degradation on the shear strength of municipal solid waste. Waste Manag. 68, 263–274.
Al Majou, H., Bruand, A., Duval, O., 2008. The use of in situ volumetric water content at field capacity to improve the prediction of soil water retention properties. Can. J. Soil Sci. 88, 533–541.
Almeida, M.S.S., Santa Maria, P.E.L., Martins, I.S.M., Spotti, A.P., Coelho, L.B.M., 2000. Consolidation of a very soft clay with vertical drains. Géotechnique 50 (6), 633–643.
Aschonitis, V.G., Antonopoulos, V.Z., Lekakis, E.H., Litskas, V.D., Kotsopoulos, S.A., Karamouzis, D.N., 2013. Estimation of field capacity for aggregated soils using changes of the water retention curve under the effects of compaction. Eur. J. Soil Sci. 64 (5), 688–698.
Babu, G.L.S., Lakshmikanthan, P., 2015. Estimation of the components of municipal solid waste settlement. Waste Manage. Res. 33 (1), 30–38.
Bareither, C.A., Benson, C.H., Edil, T.B., 2012. Compression behavior of municipal solid waste, immediate compression. J. Geotech. Geoenviron. Eng. 138 (9), 1047–1062.
Brennan, A.J., Madabhushi, S.P.G., 2010. Measurement of coefficient of consolidation during reconsolidation of liquefied sand. Geotech. Test. J. 34 (2), 102914.
Chai, J., Carter, J.P., 2011. Deformation Analysis in Soft Ground Improvement. Springer, London, pp. 247.
Chapuis, R.P., 2004. Predicting the saturated hydraulic conductivity of sand and gravel using effective diameter and void ratio. Can. Geotech. J. 41 (5), 787–795.
Chapuis, R.P., Aubertin, M., 2003. On the use of the Kozeny-Carman's equation to predict the hydraulic conductivity of a soil. Can. Geotech. J. 40 (3), 616–628.
Chiu, H.I., 2009. Effects of Leaching on Cementitious Material as Barrier and Parameter Sensitivity Analysis for Low-level Radioactive Waste Disposal. Thesis. National Central University, Taiwan.
Colangelo, F., Cioffi, R., Montagnaro, F., et al., 2012. Soluble salt removal from MSWI fly ash and its stabilization for safer disposal and recovery as road basement material. Waste Manag. 32 (6), 1179–1185.
Ecemis, N., Demirci, H.E., Karaman, M., 2015. Influence of consolidation properties on the cyclic re-liquefaction potential of sands. B. Earthq. Eng. 13 (6), 1655–1673.
Eslami, A., Fellenius, B.H., 2004. CPT and CPTu data for soil profile interpretation: review of methods and a proposed new approach. Iran. J. Sci. Technol. B 28 (B1), 69–86.
Fan, H.J., Shu, H.Y., Yang, H.S., et al., 2006. Characteristics of landfill leachates in Central Taiwan. Sci. Total Environ. 361 (1), 25–37.
Federico, A.M., Miccoli, D., Murianni, A., Vitone, C., 2018. An indirect determination of the specific gravity of soil solids. Eng. Geol. 239, 22–26.
Feng, S.J., Du, F.L., Chen, H.X., Mao, J.Z., 2017a. Centrifuge modeling of preloading consolidation and dynamic compaction in treating dredged soil. Eng. Geol. 226, 161–171.
Feng, S.J., Gao, K.W., Chen, Y.X., Li, Y., Zhang, L.M., Chen, H.X., 2017b. Geotechnical properties of municipal solid waste at Laogang landfill, China. Waste Manag. 63, 354–365.
Georgiannou, V., Coop, M., Altuhafi, F., 2018. Compression and strength characteristics of two silts of low and high plasticity. J. Geotech. Geoenviron. Eng. 144 (7), 04018041.
Holtz, R.D., Kovacs, W.D., Sheahan, T.C., 2011. An Introduction to Geotechnical Engineering. Pearson Education, Upper Saddle River, N.J.
Hossain, M.S., Penmethsa, K.K., Hoyos, L., 2009. Permeability of municipal solid waste in bioreactor landfill with degradation. Geotech. Geol. Eng. 27 (1), 43–51.
Huang, W., Fityus, S., Bishop, D., Smith, D., Sheng, D., 2006. Finite-element parametric study of the consolidation behavior of a trial embankment on soft clay. Int. J. Geomech. 6 (5), 328–341.
Jabro, J.D., Evans, R.G., Kim, Y., Iversen, W.M., 2009. Estimating in situ soil-water retention and field water capacity in two contrasting soil textures. Irrig. Sci. 27 (3), 223–229.
Jiang, J.G., Wang, J., Xu, X., et al., 2004. Heavy metal stabilization in municipal solid waste incineration flyash using heavy metal chelating agents. J. Hazard. Mater. 113 (1), 141–146.
Kim, S.U., Lim, H.D., 2012. Examination of the relationship between average particle size and shear strength of granite-derived weathered soils through 2-D distinct-element method. J. Ko. Anti-Soc. 28 (12), 77–86.

Lan, J.W., Zhan, L.T., Li, Y.C., Chen, Y.M., 2012. Impacts of initial moisture content of MSW waste on leachate generation and modified formula for predicting leachate generation. Environ. Sci. 33 (4), 1389–1396.
Long, Y., Liu, D., Xu, J., et al., 2018. Release behavior of chloride from MSW landfill simulation reactors with different operation modes. Waste Manag. 77, 350–355.
Machado, S.L., Carvalho, M.F., Vilar, O.M., 2002. Constitutive model for municipal solid waste. J. Geotech. Geoenviron. Eng. 128 (11), 940–951.
Machado, S.L., Karimpourfard, M., Shariatmadari, N., Carvalho, M.F., do Nascimento, J.C., 2010. Evaluation of the geotechnical properties of msw in two brazilian landfills. Waste Manag. 30 (12), 2579–2591.
Mesri, G., Olson, R.E., 1971. Mechanisms controlling the permeability of clays. Clay Clay Miner. 19, 151–158.
Nasta, P., Romano, N., 2016. Use of a flux-based field capacity criterion to identify effective hydraulic parameters of layered soil profiles subjected to synthetic drainage experiments. Water Resour. Res. 52 (1) (n/a-n/a).
Quina, M.J., Bordado, J.C., Quinta-Ferreira, R.M., 2008. Treatment and use of air pollution control residues from MSW incineration: an overview. Waste Manag. 28 (11), 2097–2121.
Rab, M.A., Chandra, S., Fisher, P.D., Robinson, N.J., Kitching, M., Aumann, C.D., Imhof, M., 2011. Modelling and prediction of soil water contents at field capacity and permanent wilting point of dryland cropping soils. Soil Res. 49 (5), 389–407.
Reddy, C.S., Mohanty, S., Shaik, R., 2018. Physical, chemical and geotechnical characterization of fly ash, bottom ash and municipal solid waste from Telangana state in India. Int. J. Geo-Eng. 9, 1–23.
Santra, P., Kumar, M., Kumawat, R.N., Painuli, D.K., Hati, K.M., Heuvelink, G.B.M., Batjes, N.H., 2018. Pedotransfer functions to estimate soil water content at field capacity and permanent wilting point in hot arid western India. J. Earth Syst. Sci. 127 (35), 1–16.
Sanzeni, A., Whittle, A.J., Germaine, J.T., Colleselli, F., 2012. Compression and creep of Venice lagoon sands. J. Geotech. Geoenviron. Eng. 138 (10), 1266–1276.
Shimaoka, T., Hanashima, M., 1996. Behavior of stabilized fly ashes in solid waste landfills. Waste Manag. 16 (5–6), 545–554.
Siddiqui, A.A., Powrie, W., Richards, D.J., 2013. Settlement characteristics of mechanically biologically treated wastes. J. Geotech. Geoenviron. Eng. 139 (10), 1676–1689.
Spence, R.D., Shi, C., 2005. Stabilization and Solidification of Hazardous, Radioactive and Mixed Wastes. CFC Press, Boca Raton, Florida, USA.
Stoltz, G., Gourc, J.P., Oxarango, L., 2010. Characterisation of the physico-mechanical parameters of MSW. Waste Manag. 30 (8), 1439–1449.
Su, L.J., Zhou, W.H., Chen, W.B., Jie, X., 2018. Effects of relative roughness and mean particle size on the shear strength of sand-steel interface. Meas. 122, 339–346.
Tang, Q., Liu, Y., Gu, F., Zhou, T., 2016. Solidification/stabilization of fly ash from a municipal solid waste incineration facility using Portland cement. Adv. Mat. Sci. Eng. https://doi.org/10.1155/2016/7101243.
Taylor, D.W., 1948. Fundamentals of Soil Mechanics. John Wiley & Sons, New York.
Vinod, J.S., Sridharan, A., 2015. Laboratory determination of coefficient of consolidation from pore water pressure measurement. Géotech. Lett. 5 (4), 294–298.
Wang, J.J., Zhang, H.P., Tang, S.C., et al., 2013. Effects of Particle size distribution on Shear Strength of Accumulation Soil. J. Geotech. Geoenviron. Eng. 139 (11), 1994–1997.
Wils, L., Van Impe, P., Haegeman, W., 2015. One-dimensional compression of a crushable sand in dry and wet conditions. In: International Symposium on Geomechanics from Micro to Macro. Taylor and Francis Group, London.
Xu, X.B., Zhan, T.L., Chen, Y.M., Beaven, R.P., 2014. Intrinsic and relative permeabilities of shredded municipal solid wastes from the Qizishan landfill, China. Can. Geotech. J. 51 (11), 1243–1252.
Xu, H., Zhan, L.T., Li, H., et al., 2016. Time- and stress-dependent model for predicting moisture retention capacity of high-food-waste-content municipal solid waste: based on experimental evidence. J. Zhejiang Univ. Sci. A. 17 (7), 525–540.
Yesiller, N., Hanson, J.L., Cox, J.T., Noce, D.E., 2014. Determination of specific gravity of municipal solid waste. Waste Manag. 34 (5), 848–858.
Yu, S.J., Chae, Y.S., Kim, J.K., Yoon, W.S., 2007. Effect of disturbance on the compressibility characteristics of marine clay. J. Korean Geotech. Soc. 23 (12), 95–107.
Yu, C.Y., Chow, J.K., Wang, Y.H., 2016. Pore-size changes and responses of kaolinite with different structures subject to consolidation and shearing. Eng. Geol. 202, 122–131.
Zacco, A., Borgese, L., Gianoncelli, A., et al., 2014. Review of fly ash inertisation treatments and recycling. Environ. Chem. Lett. 12 (1), 153–175.
Zeng, L.L., Hong, Z.S., Gao, Y.F., 2017. Practical estimation of compression behaviour of dredged clays with three physical parameters. Eng. Geol. 217, 102–109.
Zettl, J.D., Barbour, S.L., Huang, M., Si, B.C., Leskiw, L.A., 2011. Influence of textural layering on field capacity of coarse soils. Can. J. Soil Sci. 91, 133–147.
Zhai, Q., Rahardjo, H., Satyanaga, A., 2018. A pore-size distribution function based method for estimation of hydraulic properties of sandy soils. Eng. Geol. 246, 288–292.
Zhan, L.T., Chen, Y.M., Ling, W.A., 2008. Shear strength characterization of municipal solid waste at the Suzhou landfill, China. Eng. Geol. 97 (3), 97–111.
Zhan, L.T., Xu, H., Chen, Y.M., et al., 2017. Biochemical, hydrological and mechanical behaviors of high food waste content MSW landfill: preliminary findings from a large-scale experiment. Waste Manag. 63, 27–40.
Zhang, B., Zhou, W., Zhao, H., et al., 2016. Stabilization/solidification of lead in MSWI fly ash with mercapto functionalized dendrimer Chelator. Waste Manag. 50, 105–112.
Zhu, X.R., Xie, X.Y., Wang, Z.H., Fang, P.F., 2004. An experiment study on the geotechnical behavior of the Tianziling solid waste landfill of Hangzhou. China Civil Eng. J. 37 (10), 52–58.